Journal of Sound and Vibration (1998) **217**(1), 97–111
Article No. sv981730

A STUDY OF THE DYNAMIC STRESS CONCENTRATION FACTORS OF A FLAT PLATE FOR SEA APPLICATIONS

K. SHANKAR

NASA Johnson Space Centre, *Houston*, *TX* 77058, *U.S.A.*

(*Received* 17 *September* 1997, *and in final form* 23 *April* 1998)

Statistical Energy Analysis (SEA) methods have been used to obtain the mean square vibrational energy levels of connected structures under certain conditions of coupling and excitation by random, uncorrelated forcing. Simple relationships between spatially averaged energies or velocities to stress and strain have been developed. However, the prediction of spatial variations in dynamic stress distribution at boundaries and discontinuities is more difficult and very few studies have been made in the SEA context. This paper first compares SEA predicted spatially averaged mean square stress to that of a FEA model of a simple two-plate system. Then it studies the behaviour of the dynamic stress concentration factors at the clamped boundary and also at the corner of a square hole in a flat plate at different frequency ranges using FEA models. The method used here is particulary useful for SEA applications, the stresses being normalized to unit power input. Certain assumptions for stress prediction at boundaries from SEA derived uniform stresses are also verified.

1. INTRODUCTION

Statistical Energy Analysis (SEA) methods are increasingly used to predict the mean square response (averaged over space and time) of connected structures subjected to random rain-on-the-roof type of excitation and certain conditions of inter-structural coupling, resulting in a diffuse wave field. SEA is an energy response model, the fundamental variable being the time averaged energy of vibration. Indeed, one of the attractions of using energy as a primary variable is the ability to work out simple expressions for the mean square velocities and strains from kinetic and strain–energy equations. Several simple relations for deriving spatially averaged velocity, pressure and strain responses from energy levels of uniform homogenous structures are discussed in Lyon and DeJong [1].

The theoretical foundations of SEA and the extent and validity of the many SEA assumptions are not yet fully understood and still a subject of ongoing research. For example, in Dimitriadis and Pierce [2], the requirement of weak coupling between structures considered necessary for the application of SEA has been investigated for a system of plates rigidly joined along an edge and found not critical. Hence, the concept of structural coupling defined as a barrier to the

0022–460X/98/410097 + 15 $30.00/0

transfer of vibrational energy between subsystems, rather than "weak" or "strong", is now more appropriate from the point of view of SEA. An extensive overview of the limitations and criticisms of SEA are presented by Fahy [3]; the study lists a number of deficient areas requiring more investigation. Chief among them are the effects of coupling strength, modal overlap, indirect coupling loss factors (CLFs), transient power input, periodicity of structures, damped coupling and the spatial variation of responses.

This paper is concerned with the spatial variation of stress response, i.e., stress concentrations, at the corners of a hole or clamped edges of a flat plate and their frequency dependent behaviour. The current analysis being conducted at this NASA Centre on the dynamic response of the International Space Station (ISS) structure, involves the use of SEA methods and the prediction of stresses in flat and curved panels from SEA predicted energy levels. However, there is a need to better understand the effect of cutouts, corners and other boundary conditions in causing variations in the spatial stress distribution, in order to avoid failure of malfunction of that component. Application of the simple "stress doubling rule" of SEA mentioned later in this section is often resorted to, however, a better understanding of the limitations of this rule and the deviations from it due to effects of wavelength and size of the hole is desirable, to have confidence in its predictions. Hence, the numerical simulation (using an FEA package) of a plate with a square cutout is resorted to here and results presented in non-dimensional form to enhance the application of SEA from predicting the average stresses to understanding local stress concentrations.

The spatial variance of SEA response variables in uniform structures have been studied by Stearn [4]. Expressions for the upper and lower bounds of the normalized deviation, i.e., the ration of standard deviation to mean, of uniform flat plates and cylinders are found to be of the form $C/\sqrt{N}$, where C is a constant and N the number of excited modes. Norton and Fahy [5] conducted experiments on the mean square velocities and strain of small diameter cylinders representative of industrial pipeline systems. The simple relationships mentioned earlier in this section were used to predict spatially averaged RMS strains, then the ratio of the predicted to measured strains were plotted for a range of frequencies and modal densities. It is observed that the higher the modal densities and the smaller the wavelength of vibration the more acceptable agreement is obtained with the theoretical values of spatially averaged stresses.

The so-called response variables of SEA discussed above refer to spatial averages significantly away from the boundaries and generally deal with uniform structures. However, near the boundaries and certain discontinuities, the responses can be expected to be biased from the average. From a modal point of view, this can be explained as the concentration of anti-nodes or nodes at the free or clamped edge of a structure whereas the interior space includes both anti-nodes and nodes. The concentration of SEA responses such as stress and velocity along the boundaries are expressed as "response concentration factors", this paper being concerned about the behaviour of stress concentration factor. There can also be "modal concentration factors" in certain frequency bands due to coherence

between modes. However, if the excitation is broad-band, these are reduced substantially.

For the prediction of spatial variation of stresses, consistent with the simplicity of the SEA approach, a doubling of the mean square stress for every constrained boundary is recommended [1]. For example, at a rigidly clamped boundary (having both rotary and translatory constraints) the mean square peak stress must be four times the spatially averaged stress and at a clamped corner (the junction of two edges) there is a further doubling, i.e., a total factor of 8. The respective stress concentrations are given by square roots, i.e., 2 and 2·8. However, as shown in reference [5], in the testing of constrained pipes, the measured concentration factors at discontinuities are dependent on the wavelength of the excitation and the implications of assigning a constant value, as the above rule suggests, requires further studies.

The exact analysis of dynamic stress concentration is rendered difficult due to the complex behaviour of stress waves arriving at a boundary. Stearn [6] studies the case of concentration of dynamic stress due to a change in area of an infinite flat plate. Depending on its angle of incidence with a junction, a bending wave may be subjected to partial or total reflection, the resulting interference leading to stress concentration. Under SEA assumptions of a diffuse wave field, waves are incident from all angles and is it required to numerically integrate the stress equation over a range of incident angles for each change of thickness; the method yields a stress concentration factor which is a combination of four ''concentration'' factors dur to partial and total reflection, transmission and non-transmission. Such wave based studies which deal directly with the reflection and transmission of waves at junctions are presented by Cremer *et al*. [7] and are rather complex except for the simple geometry changes, due to the conversion of one wave-type to many others caused by mechanisms of reflection and transmission.

Pan *et al*. [8] use numerical simulations of finite beams subjected to different boundary conditions and study the spatial variation in dynamic stress. It is shown that their spatial distribution depends on the driving force location, characteristics and the mode shapes. The observation is made that, when the forcing is of flat spectrum type, the mode shapes and the location of forcing influence stress distributions; otherwise, the distribution of responses are controlled by the variations in the forcing spectrum, the former being easier to predict from a knowledge of boundary conditions.

2. STRESS COMPARISON BETWEEN FEA AND SEA MODELS OF A TWO-PLATE SYSTEM

In this section, the spatial and time averaged stress levels of a system of two plates joined at right angles and subjected to unit power input are calculated using SEA and FEA models and compared. The purpose of this comparison is to verify the procedure used to study the dynamic stress concentrations later in this paper. It may be noted that when comparing stress levels predicted by SEA and FEA, it is important to normalize the FEA stresses to the same input power as used in the SEA model (in this case, unity).

The physical properties of the plates are: area $(A) = 1 \times 1$ m, thickness $(t) = 1$ mm, modulus of elasticity $(D) = 2{\cdot}0 \times 10^{11}$ N/m^2, density $(\rho) = 7890$ kg/m^3 and the Poisson ratio $(\mu) = 0{\cdot}3$.

2.1. SEA CALCULATIONS

The SEA calculations consist of calculating the frequency dependent coupling loss factors (CLFs) and using them to obtain the time and spatially averaged energy levels, from which the mean square stresses are derived. The following calculations are based on reference [1]. Although the stresses predicted by SEA theory are approximate, the configuration of a simple two-plate system used here is a classic case of application of SEA theory; not only has it been extensively studied from the point of SEA theory but also widely used as a benchmark for experimental and finite element studies provided the necessary conditions such as rain-on-the-roof forcing are correctly simulated.

The average frequency spacing (δf) of a two-dimensional flat plate in pure bending is given by $\delta f = 2\kappa C_L/A$, where κ is the radius of gyration, C_L is the longitudinal wave speed. These are obtained by $\kappa = t/\sqrt{12}$ and $C_L = \sqrt{D/\rho(1-\mu^2)}$.

The modal overlap factor (MOF) at any frequency f can be calculated using $MOF(f) = \eta f/\delta f$, knowing the damping loss factor η. The value of η is taken as 0·04 as it is the minimum (lightest) damping to give MOFs greater than unity in the entire frequency range of interest.

The general expression for the coupling loss factor for a line connected system, of two coupled plates [1] is represented as a multiple of the normal incidence transmission coefficient $\tau(0)$ (after averaging the exact expression over incident angles from 0 to $\pi/2$, assuming that energy is uniformly distributed over incident angle),

$$\eta_{12}(f) = \frac{\delta f}{\pi f} I_{12}(k_1, k_2)\, \frac{\tau_{12}(0)}{2 - \tau_{12}(0)}, \tag{1}$$

where

$$I_{12} = \frac{L}{4}\left[\frac{k_1^4 k_2^4}{k_1^4 + k_2^4}\right]^{1/4}. \tag{2}$$

Here k_1 and k_2 are the wavenumbers at any frequency and L the length of the joint; for a symmetric plate $k_1 = k_2 = \sqrt{\omega/\kappa C_L}$ and $I_{12} = 0{\cdot}2\, L\, k_1$, and the zero incidence transmission coefficient $\tau_{12}(0)$ is 0·5.

The parameters from equations (2) and (3) are evaluated first and substituted into equation (1) to obtain the CLFs (η_{12} and η_{21}) for each frequency. The SEA equations,

$$\begin{Bmatrix} P_1 \\ P_2 \end{Bmatrix} = \begin{bmatrix} \eta_{11} - \eta_{21} \\ -\eta_{12}\eta_{22} \end{bmatrix} \begin{Bmatrix} E_1 \\ E_2 \end{Bmatrix}, \tag{3}$$

where P_1 and P_2 are the input powers (both set to unity) and the η's represent the loss factor terms, are used to calculate the time and spatial average energy levels E_1 and E_2 which are of course equal due to the symmetric forcing and geometry.

According to reference [1], the mean square tensile strain across a section of a plate of energy E and total mass M, $\langle\varepsilon^2\rangle$, is given by

$$\langle\varepsilon^2\rangle = \langle v^2\rangle/C_L^2, \qquad \langle v^2\rangle = E/M, \tag{4}$$

the maximum strain on the top and bottom fibres being $3\langle\varepsilon^2\rangle$ and the corresponding mean square stress is given by $\langle\sigma^2\rangle = 3D^2\langle\varepsilon^2\rangle$.

Values of the modal overlap factor, CLF and the square root of $\langle\sigma^2\rangle$ are calculated and plotted in the 100–200 Hz range in Figure 1.

2.2. FEA CALCULATIONS

The FEA model of two plates (each 1×1 m) coupled at right angles consisted of 450 quadrilateral plate elements (ANSYS53 Shell-63) and 496 nodes. This was within keeping with the solver capacity dictated by the memory limitations of the computer. The element dimensions were $0{\cdot}067 \times 0{\cdot}067$ m, i.e., each side of a plate being divided into 15 square elements. The nodes were constrained to prevent inplane translational and rotary motions. The frequency range of interest is 100–200 Hz.

The bending wavespeed (C_b) of an isotropic flat plate is given by

$$C_b = \sqrt{\omega\kappa C_L} = \sqrt{1{\cdot}8C_L tf}, \tag{5}$$

and the wave speed at $f = 200$ Hz is 43·7 m/s with a wavelength (λ_B) of 0·22 m which is about three times the length of an element and thus assures sufficient modal accuracy up to that frequency limit. Hence, the study is confined to the 200 Hz upper limit.

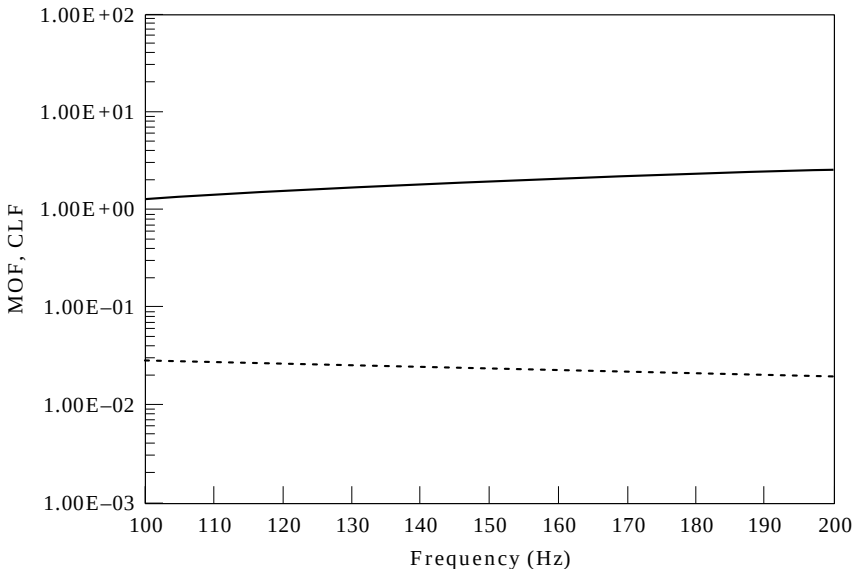

Figure 1. SEA—modal overlap factor and coupling loss factor; —, MOF; - - - , CLF.

The equation for the x-stress (σ_x) at a point x, z on a flat isotropic plate due to a pure bending displacement is given by [6]

$$\sigma_x = \frac{itD}{2(1-\mu^2)\omega}\left[\frac{\partial^2 y}{\partial x^2} + \mu\frac{\partial^2 y}{\partial z^2}\right], \tag{6}$$

where from a modal point of view, the response of the system can be written as

$$y(x, z, t) = \sum_{j=1}^{N} \phi_j(x, z)\psi_j(t), \tag{7}$$

where $\phi_j(x, z)$ is the normal mode j at (x, z) and $\psi_j(t)$, the generalized displacement of mode j. The substitution of equation (7) into equation (6) gives the so-called modal stresses $\overline{\phi}_j(x, z)$, used in the modal summation approach by FEA packages. The ANSYS53 post-processor calculates the response power spectral densities of the stress using the transfer functions of single-degree-of-freedom systems, $H(\omega)$. The general form of equation [9] giving the stress $X(\omega)_i$ at the ith degree-of-freedom due to an input cross spectral density $Y(\omega)_{lm}$ between nodes l and m is given by

$$X(\omega)_i = \sum_{j=1}^{N}\sum_{k=1}^{N} \overline{\phi}_{ij}\overline{\phi}_{ik}\left[\sum_{l=1}^{r}\sum_{m=1}^{r} \gamma_{lj}\gamma_{mk}H_j^*(\omega)H_k(\omega)Y_{lm}(\omega)\right]. \tag{8}$$

Here, r is the total number of nodes subjected to forcing, N the total number of modes, $\overline{\phi}_j$ the modal stress and γ_j the participation factor for nodal excitation for the jth mode. It may be noted that for spatially uncorrelated forcing, the cross PSDs are zero (i.e., $1 \neq m$) are zero. In this study, the normal mode summation method with 400 plate modes (ensuring satisfactory convergence) was used to calculate the mean square stress responses due to the application of many spatially uncorrelated point forces over random locations on the plate.

The use of FEA models to evaluate SEA parameters such as coupling loss factors and to check the validity of SEA results is well established. Such numerical methods are particularly suitable when studying structures having complex geometry, such as the effect of cutouts (holes) which cannot be easily analyzed by wave theory nor can the mode shapes be readily obtained analytically. Although numerical methods simplify these problems, caution must be exercised to correctly simulate rain-on-the-roof forcing and to constrain the analysis to the frequency range for which the element size is much smaller than the wavelength. The method used here to simulate random rain-on-the-roof forcing with an FEA model and obtain spatially averaged values is the same as that used by Simmons [10], Steel and Craik [11] and Shankar and Keane [12]. However, references [10–12] were primarily concerned with the extraction of SEA parameters such as CLFs from FEA models, to be used later in SEA applications. The aim here is to compare FEA responses against SEA responses obtained for unit power input, hence the

issue of normalizing the FEA stress responses to the same input power has to be dealt with. The procedure for achieving this approximately is given below.

Rain-on-the-roof forcing is simulated by subjecting a plate to point harmonic forces $\mathrm{Re}\,[F(\omega)]\,e^{i\omega t}$ of unit amplitude, acting normal to the plate surface at 25 locations chosen uniformly over the plate. As it was found that the stress produced in a plate due to excitation of the other plate, i.e., indirect forcing, were negligible compared to those caused by direct forcing, these were ignored. For the application of each force, say F_P at any point $p = 1, 2, 3, \ldots 25$, the temporal mean square values of complex x-stresses are sampled at 10 locations on the plate (i.e., $|S_1(f)|^2, |S_2(f)|^2 \ldots |S_{10}(f)|^2$) over the frequency range of interest. The average of these mean squares over the 10 locations is taken to obtain $|S_p(f)|^2$, i.e., the spatially and temporally averaged stress contribution due to the force at p. In this manner $|S_p(f)|^2$ is calculated for forcing at all points $p = 1, 2, 3, \ldots 25$ and $|S(f)|^2 = \Sigma_{p=1}^{25}|S_p(f)|^2$ gives the final averaged mean square stress caused by rain-on-the-roof forcing. Also, at each forcing point p, the normal component of the velocity ($V_p(f)$) is measured. The expression for the time averaged power input by a harmonic force is $\frac{1}{2}\mathrm{Re}\,[V_p(f)]^*$, where the asterisk denotes the complex conjugate. By summing up the absolute value of the input powers of all the 25 points, the total input power is calculated. Then the stress normalization is carried out by the equation

$$|S_N(f)|^2 = \frac{|S(f)|^2}{\sum_{n=1}^{25} [\mathrm{Re}\,[V_p(f)]^*]_{ABS}}. \tag{9}$$

3. RESULTS

The SEA modal overlap factors and CLFs are shown in Figure 1. The former are all greater than unity and increase with frequency due to the constant damping ratio model adopted here Figure 2 also shows the effect of normalizing on the root mean square FEA stress ($|S(f)|/\sqrt{2}$) and the resulting normalized stress ($|S_N(f)|/\sqrt{2}$), obtained after dividing by the total input power to the FEA model. In this case, the normalizing factor was found to be roughly constant in the frequency range and for simplicity, an average value is used through the frequency range (this is not always the case, especially in section 4 where different geometries are compared). Results here are frequency averaged over the 10 Hz bandwidth (approximately nine modes) for comparison with SEA values. The SEA predicted maximum stress (root mean square) on the top or bottom fibre of the plate section is shown in Figure 2, along with the FEA predicted stresses. There is good agreement between the SEA and FEA normalized stresses.

4. DYNAMIC STRESS CONCENTRATION FACTORS OF A FLAT PLATE

In this section, the dynamic stress concentration factors at the clamped edge of a plate and at the corner of a square hole in a plate are studied using the ANSYS53

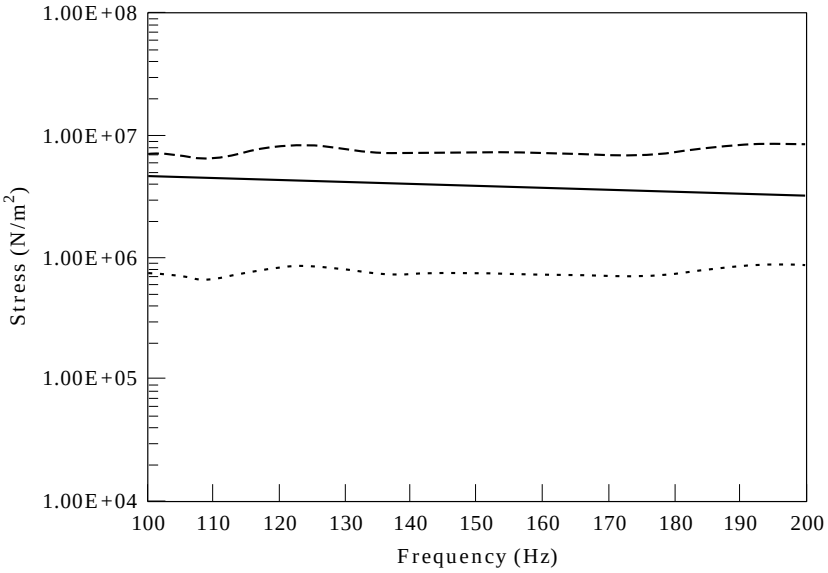

Figure 2. SEA and FEA predicted stresses: —, SEA; - - - - -, FEA normalized; . . . . . , FEA un-normalized.

package. The dynamic stress concentration factor at an edge or corner (K_{EDGE} or K_{CORNER}) is defined as

$$K = \frac{\begin{array}{c}\text{RMS value of stress at a clamped corner}\\ \text{or edge due to unit input power}\end{array}}{\begin{array}{c}\text{RMS value of stress in the datum plate}\\ \text{(spatially averaged) due to unit input power}\end{array}}, \tag{10}$$

the datum plate being a plate (without hole) of exactly the same dimensions but having free edges.

The dimensions and properties are the same as that of the plate studied in section 2. Two FEA models are used for this study; the first one being a flat plate with 693 quadrilateral plate elements (ANSYS53 Shell-63) and 744 nodes (each plate edge divided into 25 elements) and the second one being the same plate but with a square hole of dimension 0·1 × 0·1 m in the centre, with 740 quadrilateral plate elements (ANSYS53 Shell-63) and 796 nodes (see Figure 3). The first model is used to calculate the spatially averaged x-axis stresses of (1) a free–free plate, which is taken as the datum stress, and (2) at a clamped edge A (see Figure 4(a)). The second model is used to calculate the x-axis stress at a corner C or D of the hole (see Figure 4(b)) and also at the mid-point of edge B.

Using the method of equation (5), the frequency at which λ_B becomes comparable to the dimension of the elements is calculated as around 1000 Hz, which is taken as the upper limit of the current analysis. However, unlike in section 2.2, difficulties in the convergence of summation of modal stress participation factors in the high frequency ranges (due to the increasing slopes of mode shapes) necessitated using a direct solution of the dynamic stiffness equations using the

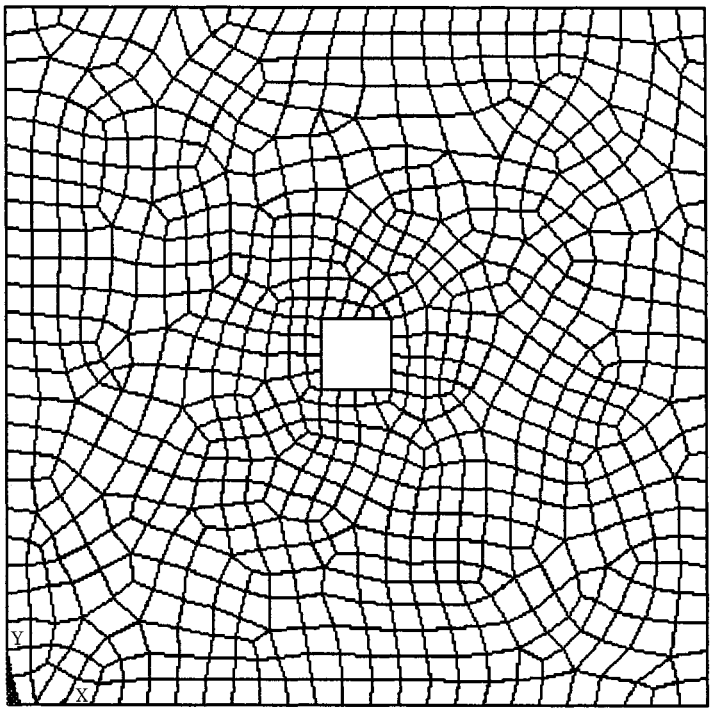

Figure 3. ANSYS53 FEA model; plate with square hole—740 elements, 796 nodes.

ANSYS53 frontal solver. This of course consumes more time, but is free from modal summation errors.

4.1. SPATIALLY AVERAGED STRESSES

First, the datum stresses are calculated as follows: the first model is given free–free boundary conditions and subjected to the same scheme of forcing as

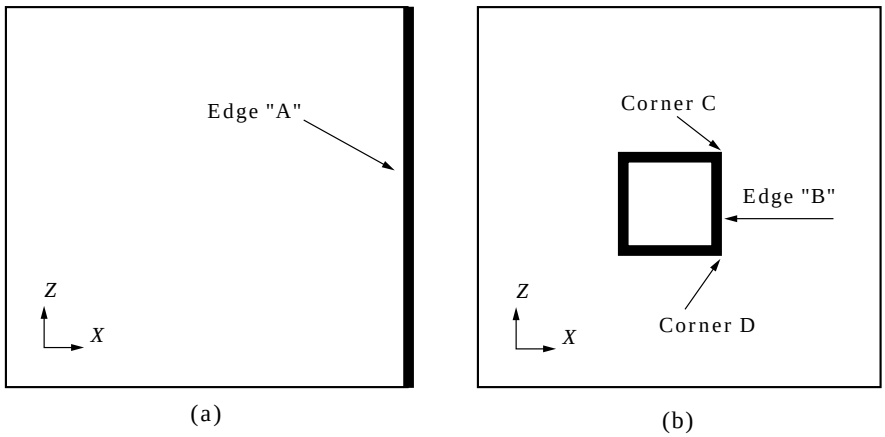

Figure 4. (a) FEA model-1: full plate with clamped or free edges; (b) FEA model-2: plate with a clamped square hole.

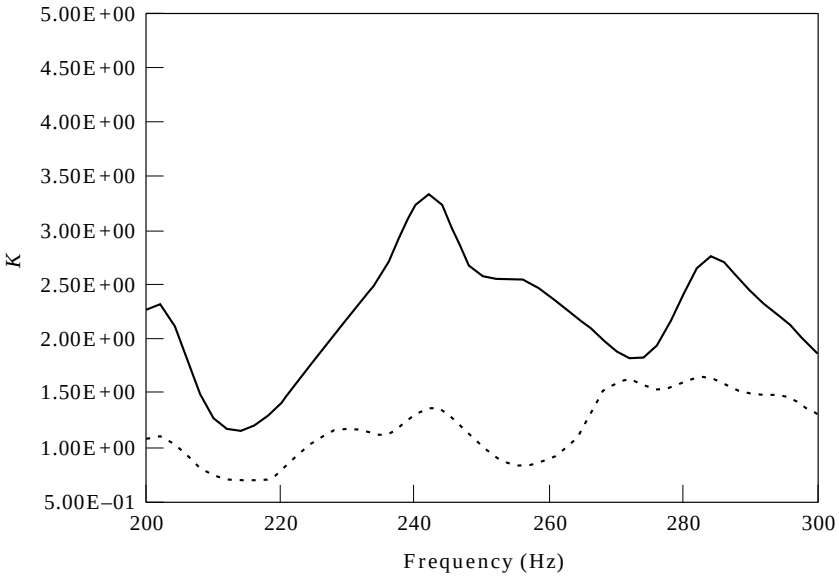

Figure 5. Dynamic stress concentration factors (K); —, K-corner; - - - , K-edge.

mentioned in section 2; then the normalized and un-normalized stresses, $|S_N(f)|_{DATUM}/\sqrt{2}$ and $|S(f)|_{DATUM}/\sqrt{2}$, are calculated. The same method is used to calculate the edge stresses $|S_N(f)|_{EDGE}/\sqrt{2}$ and $|S(f)|_{EDGE}/\sqrt{2}$, the stresses being averaged over 10 nodes along the clamped edge A. The corner stress is obtained by averaging over two adjacent corner nodes (corners C and D) of the square hole to obtain $|S_N(f)|_{CORNER}/\sqrt{2}$ and $|S(f)|_{CORNER}/\sqrt{2}$.

5. RESULTS

The variation of the normalized dynamic stress concentration factor at the corner and edge (K_{CORNER} and K_{EDGE}) with frequency are shown in Figures 5–8, their respective frequency ranges being 200–300 Hz, 420–476 Hz, 820–876 Hz and 1020–1076 Hz; the values are not frequency averaged. The ratio of λ_B/L (where L = length of a side of the plate) at the mid-frequency values of these ranges are 0·2, 0·14, 0·12, 0·11 and 0·095, respectively. The ratio λ_B/L' (where L' = length of a side of the hole) is 2·0, 1·4, 1·2, 1·1 and 0·95, respectively. The area ratio of the plate to the hole (A/A') is 100·0.

The graphs presented here are raw data i.e., not frequency averaged, in order to better study the fluctuation of stress behaviour with wavelength size at corners and edges. Values for K_{CORNER} and K_{EDGE} in the low frequency ranges are shown in Figure 5. They fluctuate with frequency, K_{EDGE} becoming less than unity in certain frequency bands. However, K_{CORNER} is always significantly greater then K_{EDGE} altough it fluctuates as well from 1·5 to 3·5. This fluctuation at low frequencies could be ascribed to the large wavelengths of the low frequency mode shapes which could cause significant differences in the drive point impedances and hence the input power at the different forcing points. In Figure 6, the curves are much smoother. Here, K_{CORNER} assumes a peak value of 2·4 and K_{EDGE} 1·7 with small

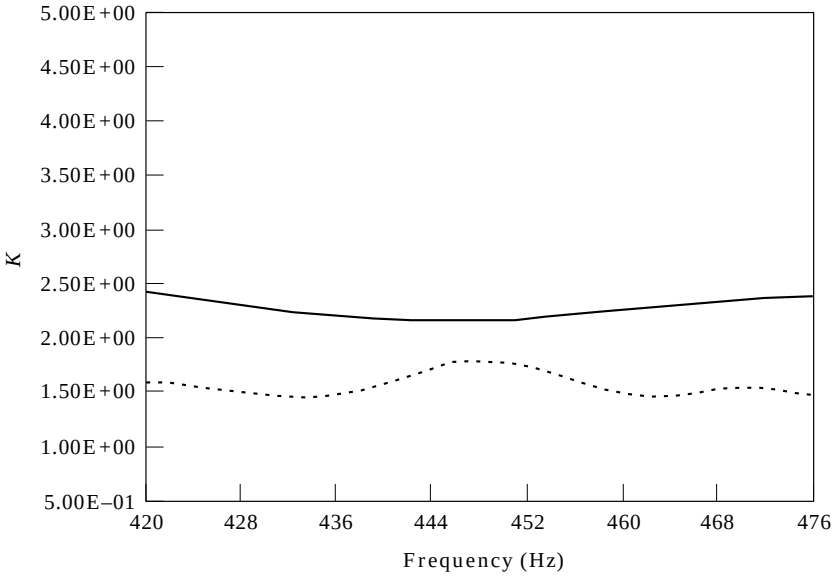

Figure 6. Dynamic stress concentration factors (K); —, K-corner; - - - , K-edge.

variations; the ratio K_{CORNER}/K_{EDGE} being around 1·5 to 1·7 (the predicted value as per the stress doubling rule being $\sqrt{2}$). At higher frequencies (see Figure 7), there is a small drop in both K_{CORNER} and K_{EDGE}, their ratio being roughly the same as above. At still higher frequencies (see Figure 8) there is a further small decrease in K_{CORNER} and K_{EDGE}, their values being around 2·2 and 1·2, respectively, the curves being very smooth and K_{EDGE} assuming a fairly constant value. Thus, it is seen that with decreasing wavelength, there is not only a small drop in the stress concentration factor, but also the curves become smoother and more constant with

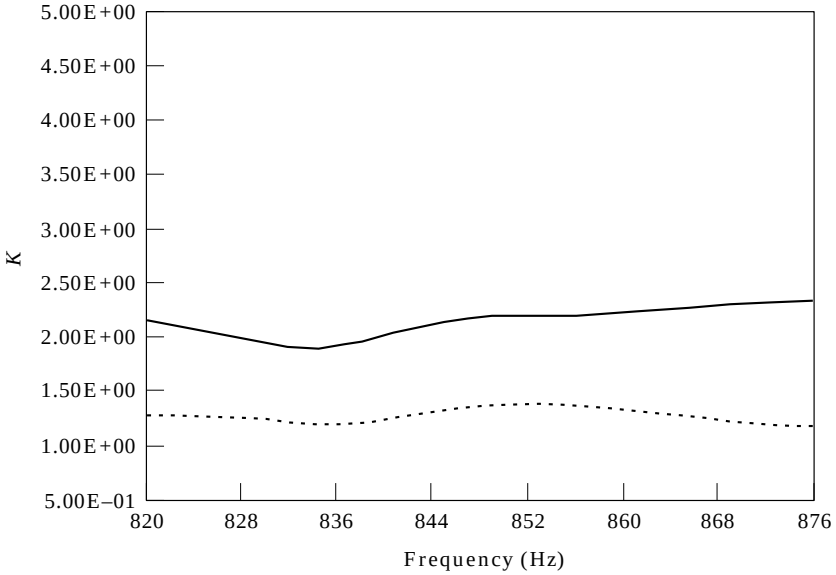

Figure 7. Dynamic stress concentration factors (K); —, K-corner; - - - , K-edge.

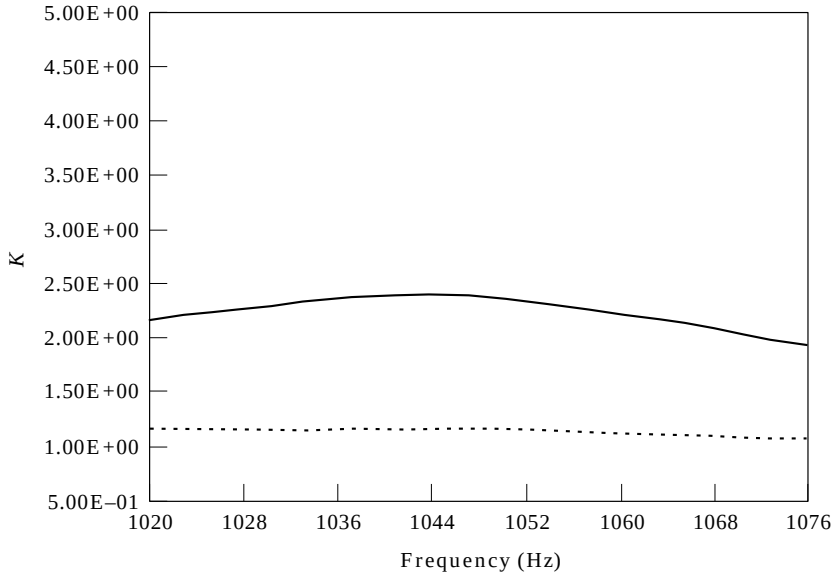

Figure 8. Dynamic stress concentration factors (K); —, K-corner; - - - , K-edge.

frequency. It may be noted that the values of stress concentration factors shown above are much less then those recommended in reference [1], i.e., the doubling of the mean square value at every constrained boundary. According to this approach, K_{CORNER} and K_{EDGE} should be taken as 2·8 and 2·0, respectively; the present study shows these to be on the safe side of stress prediction except in the very low frequency range discussed in Figure 5.

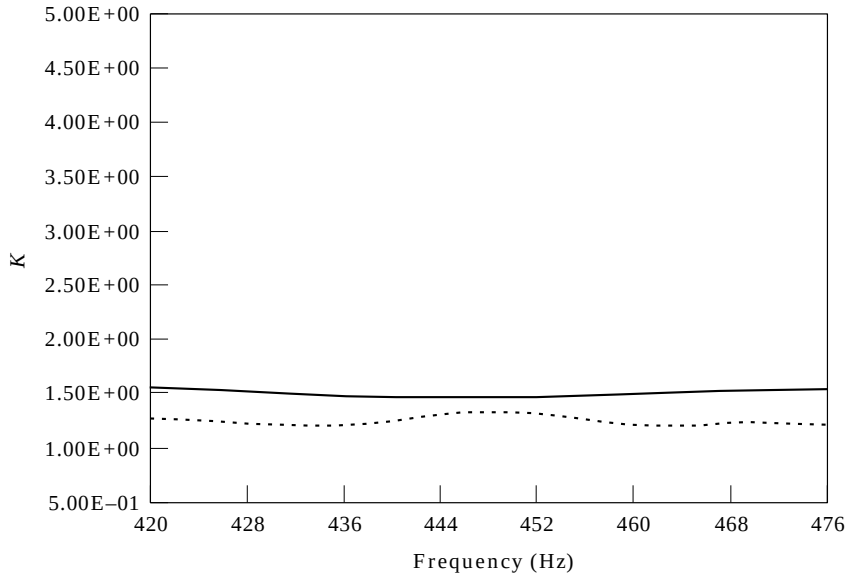

Figure 9. Un-normalized stress concentration factors (K); —, K-corner; - - - , K-edge.

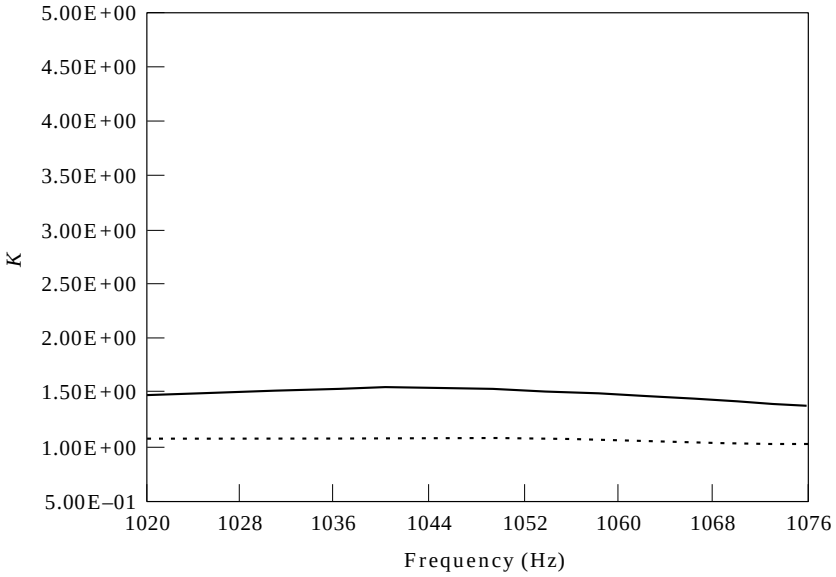

Figure 10. Un-normalized stress concentration factors (K); —, K-corner; - - - , K-edge.

The next two figures deal with K_{CORNER} and K_{EDGE} obtained without normalizing the stresses to unit input power Figures 9 and 10 deal with two frequency ranges, corresponding to $\lambda_B/L = 0{\cdot}14$ and $0{\cdot}095$, respectively. The stress concentration factors obtained are different than those with normalized stresses (Figures 5–8). The discrepancy is much more acute in K_{CORNER}, the reason being that the clamped square hole in the centre leads to significantly different geometry and boundary conditions, and hence significantly different drive point impedances and injected power from those of uniform flat plate used to calculate the datum stresses. However, in the case of K_{EDGE}, the drive point impedances far away from the clamped edge A may approximate those of the datum uniform plate leading to less significant differences in the power injected at those points. In both cases it must be expected that with decreasing λ_B/L and λ_B/L', the need to normalize the stresses decreases. The next figures (Figures 11 and 12) give K_{MID}, the normalized stress concentration at the mid-point of an edge B of the square hole, in the frequency ranges where $\lambda_B/L' = 1{\cdot}4$ and $0{\cdot}95$, respectively. It can be seen that K_{MID} is much less than unity (which implies stress relaxation) but has increased in Figure 12 compared to Figure 11 with decreasing λ_B/L'. It must be expected that with further decrease in λ_B/L' at higher frequencies, K_{MID} will increase slowly and approach the value of K_{EDGE}.

6. CONCLUSIONS

The behaviour of dynamic stresses in a flat plate with a clamped edge and then a square clamped hole, subjected to random uncorrelated forcing is studied using the ANSYS53 FEA package. The stresses are normalized to the input powers to make the results useful when studied in the context of SEA applications. There is good agreement between the SEA and FEA predicted uniform dynamic stresses

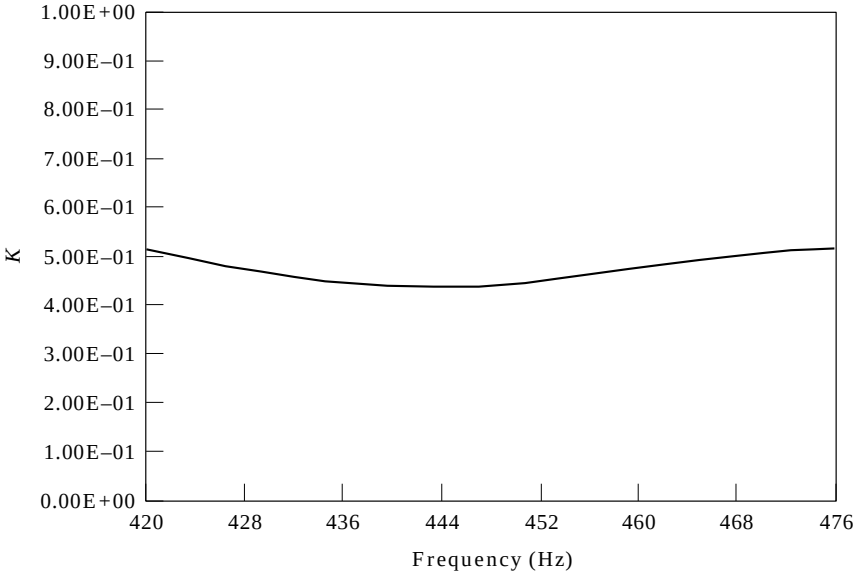

Figure 11. Mid-point stress concentration factor, K-mid, for frequency range $\lambda_B/L' = 1{\cdot}4$.

in the first part of this study. The frequency domain behaviour of the stress concentration factors K_{CORNER} and K_{EDGE} are observed. It is seen that they diminish with increasing frequency, being dependent on the relative size ofthe bending wavelength to the dimension of the fixed boundary. However, the ratio K_{CORNER}/K_{EDGE} is roughly constant and the curves are fairly smooth at high frequencies. Current recommendations given in reference [1] for estimating the spatial dynamic stress concentrations from SEA results, which call for a doubling

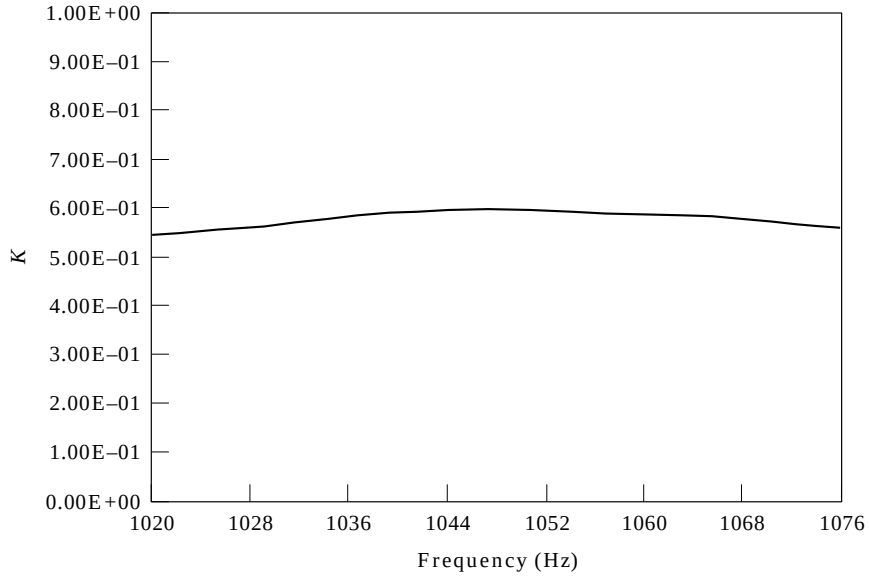

Figure 12. Mid-point stress concentration factor, K-mid, for frequency range $\lambda_B/L' = 0{\cdot}95$.

of the mean square stress at every constrained boundary, are shown to over-predict the stress concentration factors K_{CORNER} and K_{EDGE} with increasing frequency and hence to be on the safe side.

ACKNOWLEDGMENT

The author gratefully acknowledges support from the National Research Council, Washington.

REFERENCES

1. R. H. Lyon and DeJong 1995 *Theory and Application of Statistical Energy Analysis*. London: Butterworth-Heineman.
2. E. K. Dimitriadis and A. D. Pierce 1988 *Journal of Sound and Vibration* **123**, 397–412. Analytical solution for the power exchange between strongly coupled plates under random excitation.
3. F. J. Fahy 1994 *Phil Transactions*, *Royal Society of London A*, 431–447. Statistical energy analysis. a critical overview.
4. S. M. Stearn 1970 *Journal of Sound and Vibration* **12**, 85–97. Spatial variation of stress, strain and acceleration in structures subject to broadband excitation.
5. M. P. Norton and F. J. Fahy 1988 *Noise Control Engineering Journal* **30**, 107–117. Experiments on the correlation of dynamic stress and strain with pipe wall vibrations for Statistical Energy Analysis applications.
6. S. M. Stearn 1970 *Journal of Sound and Vibration* **15**, 353–365. The concentration of dynamic stress in a plate at a sharp change of section.
7. L. Cremer, M. Heckl and E. E. Ungar 1988 *Structure Borne Sound*. Berlin: Springer Verlag; second edition.
8. J. Pan, M. P. Norton and D. Karczub 1991 *Costs of Noise-Proceedings*: *Internoise*-91, **1–2**, 679–682. Australian Acoustical Society. Broad band dynamic stress concentration in finite structures.
9. ANSYS Theory Reference 1996, chapter 17, 45–48. *Spectrum Analysis*. SAS IP, Inc; seventh edition.
10. C. Simmons 1991 *Journal of Sound and Vibration* **144**, 215–227. Structure borne sound transmission through plate junctions and estimates of SEA coupling loss factors using the finite element method.
11. J. A. Steel and R. J. M. Craik 1994 *Journal of Sound and Vibration* **178**, 553–561. Statistical energy analysis of structure borne sound transmission using finite element methods.
12. K. Shankar and A. J. Keane 1997 *Journal of Sound and Vibration* **201**, 491–513. Vibrational energy flows using a substructure approach: the application of the receptance theory to FEA and SEA.